Eur. Phys. J. D **48**, 57–66 (2008)
DOI: 10.1140/epjd/e2008-00099-9

THE EUROPEAN PHYSICAL JOURNAL D

Astronomical spectrograph calibration with broad-spectrum frequency combs

D.A. Braje[1,a], M.S. Kirchner[1], S. Osterman[2], T. Fortier[1], and S.A. Diddams[1]

[1] National Institute of Standards and Technology, Time and Frequency Division, 80305 Boulder CO, USA
[2] University of Colorado, Center for Astrophysics and Space Astronomy, Boulder, CO, USA

Received 4 March 2008 / Received in final form 23 April 2008
Published online 29 May 2008 –

Abstract. Broadband femtosecond-laser frequency combs are filtered to spectrographically resolvable frequency-mode spacing, and limitations of using cavities for spectral filtering are considered. Data and theory are used to show implications relevant to spectrographic calibration of high-resolution, astronomical spectrometers.

PACS. 42.62.Eh Metrological applications; optical frequency synthesizers for precision spectroscopy – 95.55.-n Astronomical and space-research instrumentation

1 Introduction

High-resolution astronomical spectroscopy has seen rapid advancement in the last decade. Increased light gathering and instrument stability suggest the possibility of radial velocity measurements of astronomical sources down to a few centimeters per second. This unprecedented precision would enable the study of terrestrial-mass planets, improved searches for temporal variation of fundamental constants, and direct observation of the rate of expansion of the universe. While the existing astronomical wavelength standards of iodine cells and Th-Ar lamps have pushed radial velocity measurements to meters per second [1–3], their inherent limitations inhibit attaining the level of precision necessary to make the measurements listed above. An ideal wavelength standard would provide a high-density array of uniformly spaced, constant spectral brightness emission lines, the frequency of each tied to fundamental constants or to the standard SI second. In addition, the precision and long-term stability of this source should exceed the baseline of a high-resolution spectrograph. Optical frequency combs based on femtosecond lasers address all of these requirements [4,5].

Femtosecond laser frequency combs have intrinsic properties which make them enticing tools for spectrographic calibration: a broad frequency spectrum of more than an octave of bandwidth; an evenly spaced array of narrow frequency modes; the ability to stabilize both the spacing and absolute position of the comb frequencies; and long-term stability and repeatability of frequencies [6,7]. These combined attributes make femtosecond combs a near perfect frequency standard, or in essence, a consummate ruler for light frequencies. A limitation of current state-of-the-art comb technology, however, stems from the closely spaced tics of this light-frequency ruler. With typical frequency-mode spacing from 100 MHz to 1 GHz, individual comb lines cannot be easily distinguished with existing grating-based spectrographs. For precision measurements of astronomical objects, a comb spacing of 10 to 30 GHz is ideal [4]. A possible path to reaching this optimum frequency spacing leverages proven femtosecond comb technology by spectrally filtering the closely spaced comb lines. Intermediate comb modes may be suppressed by overlaying the periodic transmission function of a Fabry-Perot cavity on the more tightly spaced modes of a frequency-comb. Here we discuss cavity filtering of femtosecond-laser frequency combs for the purpose of generating a broad spectrum of resolvable lines, which can be used for astronomical spectrograph calibration.

Approaching centimeter/second resolution (equivalent to frequency shifts of tens of kilohertz in the visible spectrum) pushes the limits of stability, precision and accuracy of a calibration source. If the above measurement goal is to be reached, it will be necessary to mitigate the systematic effects of the calibration source along with those of the spectrograph and related instrumentation. We do not put forth an exhaustive list of all such issues, but instead highlight a number of parameters that warrant consideration when designing a comb-based spectrograph calibration. Cavity filtering is demonstrated by use of a ∼1 GHz Ti:sapphire laser which has been filtered by a factor of 10 and 20. The repercussions of mirror parameters, cavity refractive index, the number of filtered modes, the offset frequency, mode suppression and asymmetry, and comb

[a] e-mail: braje@nist.gov

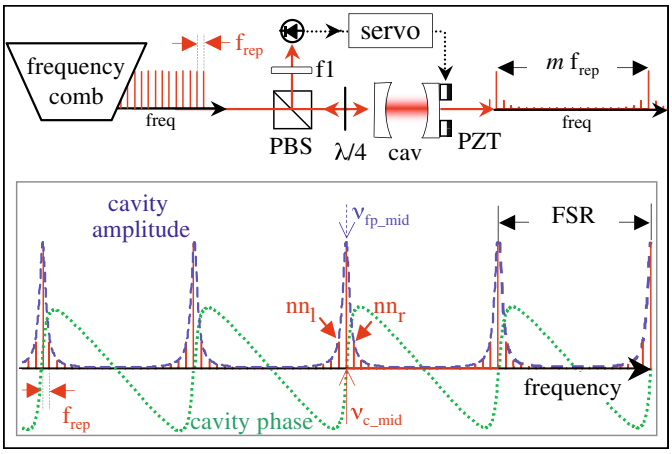

Fig. 1. (Color online) A mode-locked laser of repetition rate $f_{\rm rep}$ is filtered to a frequency-mode spacing of $mf_{\rm frep}$ by use of a Fabry-Perot cavity. The light reflected from the cavity is picked off by a polarizing beam splitter (**PBS**), passes through an optical, bandpass filter (**f1**), and serves as the input to a PZT-based servo system controlling the length of the cavity. The lower box depicts cavity amplitude (blue dashed) and phase (green dotted) that act on the electric field of the comb. An offset between the cavity and the mth comb mode is defined as $\Delta\nu_{cc} = \nu_{fp-mid} - \nu_{c-mid}$. The modes to the right and left of the mth modes are defined as the right ($\rm nn_r$) and left ($\rm nn_l$) nearest-neighbor modes.

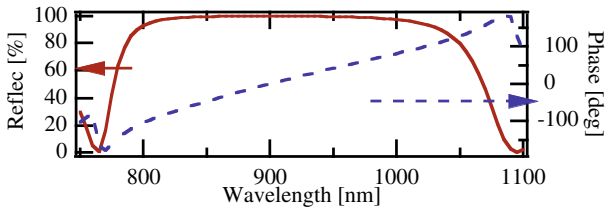

Fig. 2. (Color online) Mirror coating data provided by Ramin Lalezari of Advanced Thin Films. The phase data include the linear propagation component that is subtracted for use in calculations.

linewidth are explored. The experimental results are compared with a theoretical model, and implications of using femtosecond combs as a spectrographic calibration standard are considered.

2 Cavity filtering model

The basic principle of cavity filtering is illustrated in Figure 1. A mode-locked laser produces a comb of lines equally spaced in frequency by the repetition rate of the laser $f_{\rm rep}$ [8]. In current, state-of-the-art systems, the frequency modes are spaced too tightly to be resolved by standard astronomical spectrographs. As suggested by Sizer [9], a Fabry-Perot cavity may be used to spectrally select a set of modes from the comb that have a frequency spacing integer multiples larger than $f_{\rm rep}$. The length of the cavity is adjusted such that each cavity peak passes a comb mode that is separated from the previous cavity mode by m comb modes, thereby creating a comb with frequency spacing m times that of the input. To determine which mode has been selected, the high-repetition-rate comb may be compared with a well-known frequency standard such as Rb, I_2 or Cs for an absolute frequency calibration of the mode [10].

This straightforward concept of using a cavity to suppress intermediate frequency modes is complicated by the broad frequency range (equivalent to hundreds of nanometers) necessary for spectral calibration [11–13]. While the frequency modes of the laser are equally spaced across the entire spectrum, the cavity-mode spacing is frequency dependent. Dispersive media inside the cavity as well as phase contributions of mirror coatings cause the frequency mode spacing or free spectral range (FSR) of the cavity to vary across the spectrum. If the comb and cavity are well-overlapped at one spectral region, they walk off one another in other regions. In order to maximize the bandwidth of light transmitted through a cavity while maintaining suppression of neighboring frequency modes, the mirror reflectivity $R(\omega)$, mirror phase $\phi_r(\omega)$, refractive index inside the cavity $n(\omega)$, and frequency shift $\Delta\nu_{cc}(\omega)$ between the cavity and the comb must be considered. The offset frequency $\Delta\nu_{cc}(\omega)$ is defined as the frequency shift between the peak of cavity transmission and the nearest mth comb mode at a given frequency.

In designing a large-bandwidth filter cavity that exhibits high suppression of intermediate modes, significant effects arise from the mirror coatings. For low-group-velocity-dispersion mirrors such as those in Figure 2, there is a trade-off between higher reflectivity (which increases suppression of neighboring modes) and the bandwidth over which the cavity has a uniform FSR (where the cavity can be well matched to the comb). Even small changes in cavity FSR are detrimental to the usable spectral bandwidth of the cavity. Like a Vernier scale with one metric having inconsistent spacing, the walk-off between the comb and the cavity is *cumulative*, with each successive mth comb mode slipping further from the cavity mode.

At first inspection of the mirror reflectivity in Figure 2, it appears that the mirrors' coatings have bandwidths of a few hundred nanometers. When accounting for the phase introduced by the dielectric mirrors which comprise the cavity, the bandwidth over which the cavity can properly filter the comb is much less than the region with acceptable reflectivity. We can approximate the effect of mirror phase of highly reflective mirrors by assuming the phase is linear in wavelength and the index inside the cavity is unity. The maximum phase that can be tolerated while maintaining cavity transmission $I_{\rm out}/I_{\rm in} \geqslant 0.5$ is $|\Phi| \lesssim \sqrt{(R-1)^2/R}$. Note that Φ refers to the difference in mirror phase across the total usable bandwidth beyond the linear phase acquired due to normal propagation. In actuality, the mirror phase may oscillate between positive and negative values until the cumulative phase exceeds that of the above expression. Here we can neglect the Gouy phase shift, which has negligible frequency dependence. Using the above expression and the mirror phase

in Figure 2, a cavity bandwidth of ∼175 nm centered at 800 nm should be achievable.

When the cumulative mirror phase is small, such as for specially designed coatings or for metal mirrors, the index of refraction of air inside the cavity can become the dominant term affecting usable bandwidth. To estimate the effect of the index of air, we assume a linear variation of the index as a function of wavelength within the cavity (a reasonable approximation for air in the visible spectrum). The bandwidth $\Delta\lambda$ over which comb transmission $\geqslant$50% is limited by the change in refractive index (Δn) as $\Delta\lambda \lesssim 2\, mn\lambda^2 f_{\rm rep}\sqrt{(R-1)^2/R}/(\pi c\Delta n)$, where λ is the center wavelength of the cavity and n is the average index of refraction. The filter bandwidth varies inversely with Δn; whereas, the dependence on $f_{\rm rep}$ and m is linear. This somewhat counterintuitive linear relation stems from $f_{\rm rep}$ and m being inversely proportional to cavity length. A refractive index change of up to a few parts in 10^6 allows an optical bandwidth of the cavity of 100 nm for $m = 10$ and typical experimental parameters. If index variation becomes a concern, the cavity may be evacuated, or in certain cases, filled with a gas of known dispersion to compensate that of the mirrors.

The above equations give a terse understanding of the cavity limitations for purpose of back-of-the-envelope calculation. For a more detailed study of the cavity-comb interaction, the system is modeled by considering the electric field of all delta-function comb lines, each spaced by a frequency $f_{\rm rep}$, interacting with an air-spaced Fabry-Perot cavity of nonabsorbing mirrors. The steady-state, planar or tilted-wave cavity equation is used to model the effect of the cavity on the amplitude and phase of each comb mode [14]:

$$\frac{E(\omega)_{\rm out}}{E(\omega)_{\rm in}} = \frac{1-R(\omega)}{1-R(\omega)e^{i[2n(\omega)\omega L/c+2\phi_r(\omega)+\phi_D]}}. \quad (1)$$

$R(\omega)$ and $\phi_r(\omega)$ account for the coefficient of reflection and phase upon reflection of the cavity mirrors. Because this is a planar derivation, ϕ_D is added empirically and considers all geometrical phase terms such as the Gouy phase ($\sim 2\cos^{-1}[1-L/r]$ where r is the radius of curvature of the cavity mirrors). The index of refraction, $n(\omega)$, is taken for that of air using the Ciddor equation [15] for typical laboratory conditions of 24 °C, 630 Torr, a fractional humidity of 30%, and 400 ppm of CO_2. The cavity length L is adjusted such that the filter cavity passes an integral number m of comb modes through each cavity FSR. Unless otherwise noted, all theoretical curves assume that the comb modes overlap the cavity modes; i.e, $\Delta\nu_{cc} = 0$ at the center of the mirror coatings $\omega_{\rm mid}$. The spectral phase of the laser as a function of frequency is assumed constant.

Modeling the cavity parameters with equation (1) reproduces the observed spectrum in both the time and frequency domains. Although cavity filtering is practical for increasing the temporal pulse rate [9,16,17] as well as for improving performance of microwave generation by optical frequency combs [18,19], here we focus on the effect of thinning the frequency modes of a laser frequency comb.

3 Experimental setup

Figure 1 depicts a schematic of the apparatus used in the experiments. A broadband, Ti:sapphire laser [20] generates a ∼1 GHz-repetition-rate, octave-spanning (550 nm-1100 nm) comb. The absolute frequency of the Nth comb mode may be written as $f_N = Nf_{\rm rep} + f_0$, where the two degrees of freedom are the carrier-envelope offset frequency f_0 and the mode spacing $f_{\rm rep}$. The repetition frequency is varied with cavity length and is easily accessible and controllable. The offset frequency is determined by leveraging the broad comb spectrum, which exceeds an octave of bandwidth. A group of modes at the red side of the spectrum is frequency-doubled and heterodyned against modes on the blue side of the laser's spectrum. The observed beat frequency corresponds to f_0 and may be controlled by adjusting the pump laser power. Both f_0 and $f_{\rm rep}$ are ultimately referenced to a hydrogen maser; the resulting spectrum consists of $\sim 10^6$ comb frequencies, equally spaced by $f_{\rm rep}$.

In order to select the spectrum of the comb which matches that of the cavity mirrors, the spectral envelope of the laser is filtered by multiple reflections from plane mirrors of the same coating as the cavity. The remaining comb spectrum is spatially mode-matched into a Fabry-Perot-filter cavity of variable length. The cavity consists of two spherical mirrors with radii of curvature 50 cm and dielectric coatings of peak reflectivity 99.2% centered at 910 nm. The light, which is reflected from the cavity, is separated from the incoming light with a polarizing beamsplitter, detected on a photodiode, and is used to stabilize the length of the cavity to an integral number of comb modes. A tunable, optical bandpass filter (f1 in Fig. 1) selects the portion of the optical spectrum used to lock the cavity length. The detected light creates an error signal, which maximizes the intensity of the cavity-transmitted modes in the spectral bandwidth of f1. This error signal drives a PZT servo system, dithered at 74 kHz, that controls the length of the cavity. The cavity length [$L \approx c/(2\ nmf_{\rm rep})$] may be scanned and then locked such that it passes m comb modes per FSR. Cavity transmission is studied for filter numbers of $m = 10$ ($L \approx 1.5$ cm) and $m = 20$ ($L \approx 0.75$ cm). Due to the frequency-dependent spatial mode of the laser, excitation of only the lowest-order cavity mode requires additional spatial filtering. To determine suppression of intermediate modes, the comb teeth that traverse the cavity in the lowest-order cavity mode are detected either with a fiber-coupled fast photodetector to obtain a RF spectrum or with a fiber-coupled, grating-based optical spectrum analyzer to measure the envelope of the optical spectrum.

4 Results

4.1 Mirror reflectivity and phase

As described above, the ideal spectrographic calibration source spans more than an octave of spectral bandwidth; however, a cavity (which is necessary to filter the dense

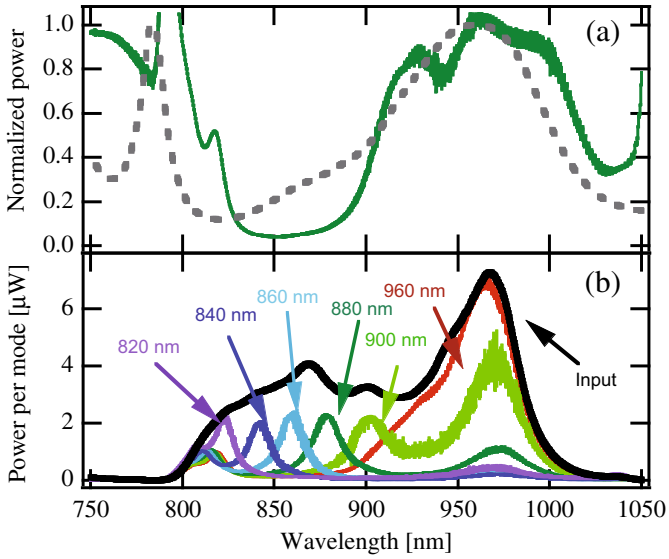

Fig. 3. (Color online) (a) Experimental (green solid) and simulated (grey dashed) transfer function ($I_{\rm out}/I_{\rm in}$) for the $m = 20$ comb modes. Cavity length is locked with filter f1 centered at 960 nm. (b) Effect of cavity lock wavelength (as determined by f1) on transmission through the cavity. Cavity-filtered spectra in power/mode as a function of wavelength are shown for a lock wavelength centered at 820 nm, 840 nm, 860 nm, 880 nm, 900 nm, and 960 nm. The input spectrum is vertically scaled by $m = 20$ to account for the suppression of intermediate modes.

spectral modes) has a limited spectral range over which its modes overlap the evenly spaced comb modes. Let us first consider how much spectral bandwidth can be transmitted through a cavity. Figure 3a depicts the experimental (green, solid) and theoretical (grey dashed) cavity-filtered spectrum normalized to the input spectrum while the cavity is locked to $L \approx 0.75$ cm to filter every 20th mode. The locking wavelength is centered at 960 nm. The experimental data are taken on a high-resolution optical spectrum analyzer with resolution bandwidth of 0.2 nm. The cavity effectively transmits nearly 100 nm of the input spectrum before the cavity modes walk off the filtered comb modes. The fuzzy appearance of the transmitted spectrum results from the optical spectrum analyzer sampling the discrete transmitted comb frequencies (and the absence of neighboring modes). The theoretical curve of the $I_{\rm out}/I_{\rm in}$ for each mth comb mode was generated by use of equation (1), experimental parameters, and mirror coatings of Figure 2. Although the mirror reflectivity bandwidth appears to cover much of the spectrum from 800–1000 nm, the transmission bandwidth from the cavity is limited by the frequency-dependent phase shift of the mirrors and cavity, as discussed above. Here the data are shown for a filter number of $m = 20$. As the length of the cavity is adjusted to filter fewer intermediate modes, the cavity mode full-width-at-half-max decreases linearly, thereby further limiting the transmitted envelope. While it may appear advantageous to filter a large number of intermediate modes when considering cavity bandwidth, suppression of nearest-neighbor modes decreases with larger m. This is discussed further in Section 4.3.

The alignment of the cavity and comb modes at the locking wavelength of the cavity also affects the relevant bandwidth of the cavity filter, as shown in Figure 3b. Here the power/mode of the comb spectra is plotted, and the input curve is scaled by $m = 20$ to account for the filtered modes. The cavity parameters are initially optimized by use of the entire spectrum, and then different optical bandpass filters (filter f1 of Fig. 1) are placed in the path of the servo detector. Optical spectra at a number of locking wavelengths are depicted. Note that the width of the envelope of the transmitted modes decreases as the cavity lock point is shifted from 960 nm. The smaller intensity of the cavity-transmitted spectrum results from increasing cavity-comb misalignment ($\Delta\nu_{cc} > 0$) at the center of the spectrum. When filtering with a single cavity, f_0 of the laser may be adjusted to match the cavity transmission peak at the center of the spectrum; however, when multiple cavities filter the comb in parallel, cavity-comb offset is difficult to eliminate for all cavities simultaneously. In the next section, we study the effect of $\Delta\nu_{cc}$ in greater detail.

4.2 Cavity-comb offset

If the offset frequency f_0 of the laser is adjusted (by changing the dispersion in the laser cavity) such that the Fabry-Perot cavity length is an exact integral number of comb modes, but cavity and comb modes do not overlap at $\omega_{\rm mid}$ (i.e, $\Delta\nu_{cc} \approx f_{\rm rep}/2$), it would seem that no light could be transmitted through the cavity. Without tuning the length of the cavity, the comb modes are not aligned with the cavity modes, and the comb is largely filtered. In practice, however, the length of the cavity may be adjusted, thereby very narrowly changing the cavity mode spacing from an integral number of comb modes; in which case, the cavity-length shift aligns the center frequency modes, but at the same time forces the cavity length to differ from an exact integral of comb modes. Figure 4 depicts theoretical curves showing the impact of a cavity-comb misalignment at the center of reflectivity of the mirror coatings. Cavity length, cavity transmission, and the width of the transmitted spectral envelope are plotted as a function of $\Delta\nu_{cc}$ at $m = 20$. To separate differing effects, the profiles assume a cavity in vacuum. Peak cavity is transmission is optimized for modes over a 20-nm bandwith at the center of reflectivity of the mirrors.

As $\Delta\nu_{cc}$ changes, the cavity length has a corresponding linear adjustment as seen in Figure 4a. This diversion from the optimal cavity length causes a corresponding decrease in the peak amplitude transmitted through the cavity. Figure 4b is plotted using the experimental mirror parameters. Higher mirror reflectivity would cause further reduction of the power through the cavity as $\Delta\nu_{cc}$ increases. For maximum transmission, the offset of the laser must be tailored to the cavity. While taking experimental data, $\Delta\nu_{cc}$ is not optimized, but the cavity length is adjusted to compensate.

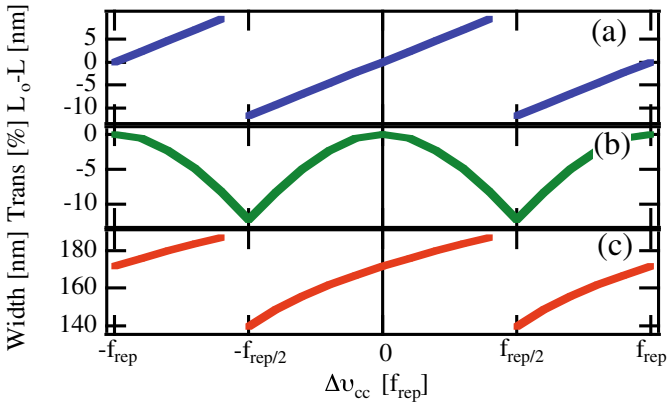

Fig. 4. (Color online) Calculation of the effect of $\Delta\nu_{cc}$ of the comb relative to the cavity for the mirror design of Figure 2. (a) As the offset shifts over the range of $f_{\rm rep}$ (1 GHz), the cavity length for optimum transmission and bandwidth vary linearly; at $\Delta\nu_{cc} = f_{\rm rep}$, the optimum alignment point shifts to the next peak in the length scan as represented by the discontinuities. (b) Less than 15% variation in cavity transmission in a 50 nm bandwidth is seen as $\Delta\nu_{cc}$ is varied. If mirrors of higher reflectivity are used, this variation increases. (c) Spectral width slightly increases as $\Delta\nu_{cc}$ increases; however, note that the increase in bandwidth is at the expense of transmission.

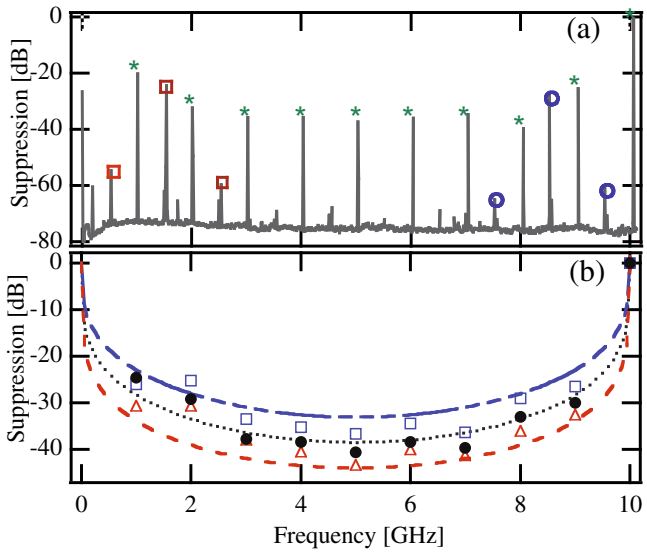

Fig. 5. (Color online) (a) Heterodyne beat note of the CW diode laser against filtered comb normalized to the mth mode. RF spectra shows both the cumulative RF beat ($*$) as well as the heterodyne ($\square$) and conjugate heterodyne ($\circ$) beat notes. (b) Cycloid-like function of cumulative mode suppression as a function of RF frequency taken with the comb locked at different wavelengths. Red triangles [920 nm], black circles [960 nm] and blue boxes [1000 nm] represent data taken in differing spectral regions. The red-dashed, black-dotted, and blue-dashed lines are theoretical simulations using experimental parameters.

It is perhaps counterintuitive that the spectral envelope (as defined by $I_{\rm out}/I_{\rm in} > 0.5$) transmitted by the cavity is slightly augmented as $\Delta\nu_{cc}$ is increased Figure 4c. The broadening in the spectral width comes at the expense of peak amplitude through the cavity in the case of vacuum. The spectral bandwidth may be further increased if a dispersive material such as a gas is used to balance the cavity walk-off.

4.3 Side-mode suppression

Until now, the discussion of functional cavity bandwidth has centered on cavity transmission. For applications such as high-precision spectrographic calibration, the definition of usable bandwidth depends just as critically on the suppression and the asymmetry of the filtered modes with respect to the mth modes. If other comb modes are not adequately suppressed, they can shift the spectral calibration causing systematic errors. For example, in a typical astronomical Echelle spectrograph with resolution $\lambda/\Delta\lambda \approx 150\,000$ and three pixel sampling, each pixel corresponds to ∼750 MHz at 900 nm. Each resolution element cannot distinguish between the mth mode and its nearest neighbors. If nn_l and nn_r are of equal intensity, the resulting frequency shift may be negligible. However, if the nearest neighbor modes are asymmetric in intensity for any reason (such as $\Delta\nu_{cc} \neq 0$ or higher order spatial modes of the cavity cause asymmetry in the cavity transmission), the calibration of the mth mode will have a frequency error Δf. Using the intensity of a transmitted mode and its unresolved nearest neighbors at the focal plane of the spectrograph, we can estimate $\Delta f \approx 2f_{\rm rep}A(I_{\mathrm{nn}_l} - I_{\mathrm{nn}_r})/(I_{\mathrm{nn}_l} + I_{\mathrm{nn}_r})$, where A is the average (linear) attenuation of I_{nn_l} and I_{nn_r}. For a suppression of 1/100 or 20 dB and an asymmetry of $I_{\mathrm{nn}_l}/I_{\mathrm{nn}_r}$ of 3:1, the line calibration shifts by 10 MHz. An equivalent Doppler velocity of 1 cm/s at 920 nm requires <10 kHz; thus, both the suppression and the asymmetry of neighboring modes must be considered.

The standard method of spectral filtering has been demonstrated by measuring the RF spectrum of the comb after the filter cavity [21]. A fast photodiode detects the cumulative RF signal of all comb modes beating against each other. For a $f_{\rm rep} = 1$ GHz laser through a $m = 10$ filter cavity, the data and theory are shown in Figure 5a by the points marked by $*$. The first peak at 1 GHz results from the vector sum of each comb mode beating with its nearest neighbors; the second peak at 2 GHz from second nearest neighbors. The RF signal at 10 GHz derives from the sum of every 10th cavity mode. Let us examine the 1 GHz beat note. Taking into account the phase of the cavity as shown in Figure 1, each 1 GHz beat note from a single comb mode against its neighbor will vary in phase from one to the next. The cumulative RF spectrum, each beat note a vector sum, may appear to have increased side-mode suppression. In the case where the comb and the cavity are not well aligned, the overestimate of suppression can be quite large. Figure 5b shows the cumulative suppression measured with the cavity locked at 920 nm, where the comb and cavity are well matched, and

at 960 nm and 1000 nm where the cavity-comb alignment degrades. The theoretical curves (solid lines) take into account the vector sum of all beat notes and provide little information regarding the asymmetry of suppression.

A more accurate measure of nearest neighbor suppression may be achieved by heterodyning the output of the filter cavity against a CW laser. Rather than considering the suppression of all $m-1$ filtered comb modes, here we are concerned only with the largest side modes. Due to the Airy function amplitude of the filter cavity, the modes which are least suppressed are those directly neighboring the mth comb modes. Figure 1 defines the left- and right-nearest-neighbor frequency modes ($\mathrm{nn_l}$ and $\mathrm{nn_r}$) at the center frequency of the spectrum. Because $\mathrm{nn_l}$ and $\mathrm{nn_r}$ modes have the least suppression of the filtered modes (unless the cavity and comb are completely misaligned), a more meaningful figure of merit of the usable bandwidth may be defined by the suppression of these modes. Using equation (1) for the amplitude of the filtered modes with respect to the mth transmitted mode, the suppression S [in dB] of the kth sideband is:

$$S = 10\log\left[\frac{R^2 - 2R\cos\left(2\pi\dfrac{\Delta\nu_{cc}}{mf_{\mathrm{rep}}}\right)+1}{R^2 - 2R\cos\left[2\pi\left(\dfrac{\Delta\nu_{cc}}{mf_{\mathrm{rep}}}+\dfrac{k}{m}\right)\right]+1}\right] \quad (2)$$

where $k = \pm 1$ refers to the nearest neighbor modes. Note that $|k| < (\lfloor m/2 \rfloor - 1)$ for suppression of the kth sideband with respect to its nearest mth mode. The expected suppression of the nearest neighbor modes on a single pass through the cavity may be obtained by setting $\Delta\nu_{cc} = 0$. Note that higher suppression is attained as fewer modes are filtered. The ratio of equation (2) with $k = 1$ to that with $k = -1$ provides an estimate of side mode asymmetry. Although calculation of the lowest order spatial mode of the cavity does not predict significant asymmetry of suppressed modes, higher order spatial modes enter asymmetrically and can be problematic.

The beat notes marked by □ in Figure 5a denote the RF frequencies resulting from a ∼4 mW CW diode laser at 960 nm beating against the mth comb tooth. The heterodyne laser and filtered comb are combined in a fiber-based beamsplitter, which spatially overlaps the filtered comb and the CW laser. The highest □ peak results from a heterodyne laser, which is detuned by 1.8 GHz from the nearest transmitted comb mode. This 1.8 GHz offset is chosen in order to separate the heterodyne measurement from the cumulative peaks (∗), which occur in multiples of f_{rep} and are always present. By measuring the suppression of the right and left (□) beat notes against the peak, any asymmetry in suppression of nearest neighbors ($\mathrm{nn_l}$ and $\mathrm{nn_r}$) may be derived. Due to the repetitive nature of the comb, a conjugate beat of the heterodyne laser against the next mth cavity mode is also present. The conjugate beat note of the laser at 8.2 GHz ($f_{\mathrm{rep}} - 1.8$ GHz) is marked with ∘. Again, the lower marked peaks correspond to the nearest neighbor modes, and the suppression of each may be directly measured.

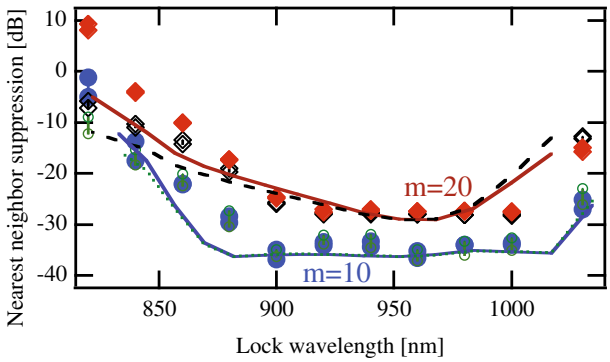

Fig. 6. (Color online) Data are plotted by measuring the suppression of the $\mathrm{nn_l}$ and $\mathrm{nn_r}$ at each of the locking bandwidths. Black open (◊) and red filled (♦) diamonds are the suppression of $\mathrm{nn_l}$ and $\mathrm{nn_r}$ at $m = 20$, and green open (∘) and blue (•) circles are for $m = 10$. The solid lines represent the theoretical curves for right (solid line) and left (dashed line) nearest neighbors.

To use the filtered comb as calibration source, it is necessary to determine side-mode suppression as a function of wavelength. Tuning a heterodyne laser across the entire transmitted cavity spectrum would allow measurement of both suppression and asymmetry. Because the frequency of our heterodyne laser is fixed, we instead shift the cavity locking wavelength by changing f1 in Figure 1. Figure 6 shows the theoretical and experimental curves at $m = 10$ (∘ and •) and $m = 20$ (◊ and ♦) for the suppression of $\mathrm{nn_l}$ and $\mathrm{nn_r}$. The simulated curves take into account the full theoretical model where the length of the cavity is adjusted as a free parameter. Both $m = 10$ and $m = 20$ show similar dependence upon locking wavelength; however, suppression is greater for fewer intermediate modes. In a high-resolution spectrograph where side-mode suppression can cause an apparent shift in calibration, the limiting factor for the usable spectral bandwidth of the cavity results from both the suppression of the side modes as well as from the asymmetry of the suppressed modes.

4.4 Filtering an octave of comb bandwidth

Use of a frequency comb for astronomical spectrograph calibration requires (1) a large spectral bandwidth, (2) frequency modes spaced by 10–30 GHz, and (3) high suppression (>27 dB or a signal to noise of 500) of neighboring modes for velocity calibrations accurate to cm/s [4]. These combined requirements are unphysical for a single filter cavity with our current coatings; however, multiple cavities in parallel allow coverage over the entire spectrum [5]. As depicted in Figure 7, the comb spectrum may be split into functional spectral bandwidths by use of dichroic mirrors. Each cavity (c1-c4) filters the comb to mf_{rep}, and the filtered combs are recombined. The final mirror, $\mathrm{M_{fil}}$, may be designed to spectrally flatten the comb output. In place of $\mathrm{M_{fil}}$, a grating/spatial light modulator system could be used. Although the filtered frequencies of each cavity are

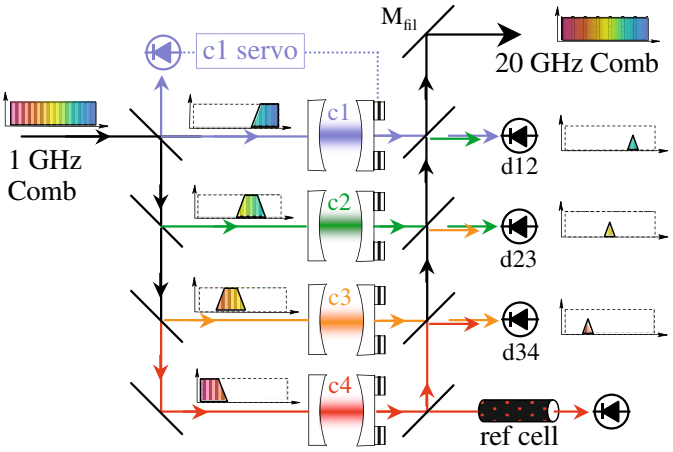

Fig. 7. (Color online) Because a single cavity with mirror coatings of Figure 2 cannot filter a wide spectrum, the comb is spectrally divided among a number of filter cavities. Cavities (c1-c4) process the spectrum in parallel, each cavity filtering a portion of the spectrum to the necessary frequency-mode spacing. The length of individual cavities is stabilized by a PZT. One cavity is referenced to an absolute frequency, and the offset between the remaining cavities (an integral of $f_{\rm rep}$) is monitored with detectors (d12, d23, d34).

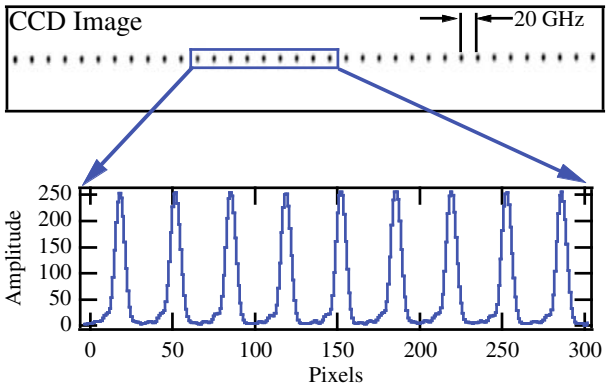

Fig. 8. (Color online) CCD image of a 1 GHz Mode-locked laser filtered to 20 GHz by a cavity and then spectrally dispersed with a grating. The plot is an intensity profile of a subsection of lines.

spaced by $mf_{\rm rep}$, the cavities may have a frequency offset. For example, cavity c1 may filter the m modes over the blue wavelengths while cavity c2 could pass the $m+5$ modes in the green (i.e. both cavities have a filter number m, but are offset from one another in an overlapping spectral region by $5f_{\rm rep}$). This offset between cavities can be used to reference one cavity to the next. By use of a reference cell in combination with the stabilized $f_{\rm rep}$ and f_0 to determine the absolute frequency offset of the first cavity, an absolute frequency reference for all filtered modes may be determined.

The offset of each cavity with respect to the next may be designed directly into the mirror coatings, or more practically, a slight change in cavity length may be used at the expense of cavity transmission bandwidth. For more control, a gas of known index may be used in combination with a small change in the length of the cavity.

5 Spectrograph calibration

Up to this point, we have considered the frequency filtering of comb modes to spectrographically resolvable frequency spacing while maintaining suppression of the neighboring frequency modes. For this comb to be a useful calibration source, we must also address precision. Although the constant spacing of the comb lines has been demonstrated, many factors can create an apparent shift of the center of gravity (COG) of the comb lines.

Figure 8 shows an image of 35 comb lines that have been filtered by a 20 GHz cavity, dispersed by a high-resolution grating, and imaged onto a charged-coupled device (CCD) camera. The graph plots a subset of CCD pixels as a function of intensity and shows nine of these comb lines. For a standard spectrographic calibration, the data would be fit with nine individual Gaussian functions (or an instrument point spread function), each with amplitude, width, position, and offset. The strength of using a comb to calibrate the spectrograph lies in the ability to leverage the equally spaced frequency components. If the dispersion solution of the spectrograph is unknown, the color centers of the comb can be individually fit in order to obtain an accurate calibration. In the simplest case of a linear relation at the focal plane of the spectrograph, the entire spectrum may be fit with a sum over j Gaussians, equally spaced along x in place of j Gaussians, each with four free parameters. Here the sum $\sum_j a\exp[-(x-bj-d)^2/c^2]+e$ uses a total of five free parameters for the entire comb, proportional to the: peak a, separation b, width c, uniform shift d, and noise floor e. Because we can assume constant spacing, the fit is less sensitive to parameters such as asymmetric suppression of nearest-neighbor modes. Small errors that would typically cause an apparent shift in the center of gravity of one calibration point are now averaged, and the fit with fewer free parameters has a tighter confidence interval.

Although calibration in this manner does reduce some systematic errors, the properties of the comb itself must be considered. In the above calculations, the comb lines were assumed to be infinitely narrow. Under this premise, the filter cavity acts on the amplitude of a delta function, and no COG shift is possible. In a physical comb system, the frequency reference, which is used to stabilize the comb, contributes to a *frequency-dependent linewidth* of the comb teeth. When the comb is locked, the frequency modes of the laser may be modeled as a Gaussian with a finite full width at half max, $\nu_{\rm L}(\omega)$. If the cavity and comb modes are perfectly overlapped, the cavity slightly reshapes the comb mode, but does not shift the COG. As the cavity and comb slip off one another, the cavity asymmetrically reshapes the comb teeth, thereby giving the appearance of a frequency shift. The larger the ratio of comb tooth width to the cavity width, the greater the

shift in COG. In the limit where the width of a comb tooth exceeds that of the cavity, the cavity function completely reshapes the comb mode, and there is a 1:1 ratio between the COG shift of the comb line and $\Delta\nu_{cc}$. This systematic error, which develops from cavity filtering of the mth mode, would be carried through the spectrograph, creating an apparent shift in calibration.

Here we are discussing the shift of the line COG before the spectrograph. An additional shift will occur at the focal plane of the spectrograph due to the asymmetry and suppression of the unresolved nearest neighbor modes. Figure 9 plots the COG shift due to cavity filtering as a function of the offset between cavity and comb for $m = 20$ (a) and $m = 10$ (b). These curves are plotted for a mirror reflectivity of $R = 0.99$. On the upper axis, equation (2), is used to give a guideline for the suppression of the nearest neighbor with respect to the mth comb mode. The combination of necessary suppression and maximum tolerable shift in COG determine the allowed linewidth of the comb modes. In a cavity of $R = 0.99$ and $m = 10$, which results in a cavity full-width at half-max of 32 MHz, a comb linewidth of $\Delta\nu_{\rm L} = 1$ MHz has less than 20 kHz shift of the COG while suppression is better than 30 dB. With this level of stabilization, spectroscopic calibrations on the level of a few centimeters per second are possible. For cavity mirrors with reflectivity greater than 99%, the shift in COG is greater than that plotted in Figure 9.

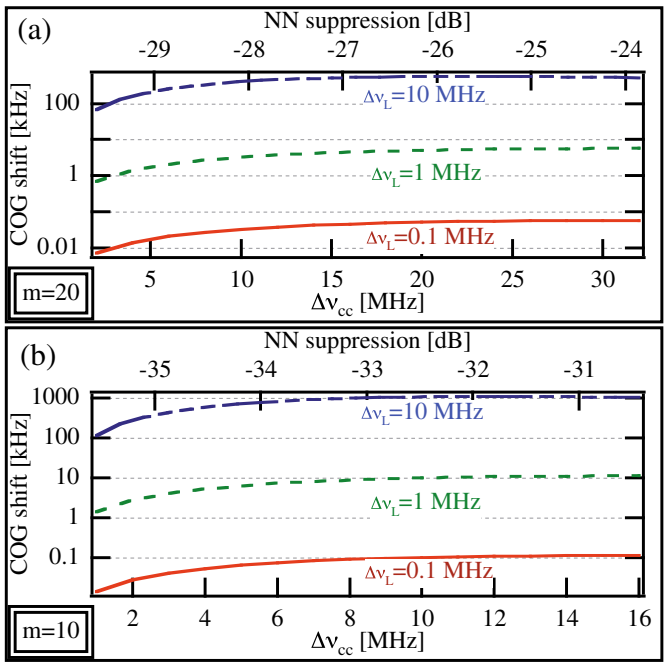

Fig. 9. (Color online) Apparent COG shift of a filtered comb line as a function of the offset between the cavity and a comb mode. Suppression of the nearest neighbor mode relative to the central peak is given as a guideline on the upper axis. The shift is plotted for $R = 0.99$ and $\Delta\nu_{\rm L}$ of 0.1 MHz, 1 MHz, and 10 MHz. Filter numbers of $m = 20$ and $m = 10$ are shown in (a) and (b), respectively. For a $f_{\rm rep} = 1$ GHz comb and $R = 0.99$, this corresponds to a cavity linewidth of 64 MHz at $m = 20$ and 32 MHz at $m = 10$. At ∼800 nm, a shift of 12.5 kHz is equivalent to a radial velocity of 1 cm/s.

Depending on the level of precision necessary for spectrograph calibration, various frequency references may be used to stabilize the comb. A practical and relatively inexpensive option is a low-noise quartz oscillator (typically 5 or 10 MHz) that has its frequency steered on intermediate time scales to a compact microwave atomic standard (such as Rb). On longer time scales the accuracy of the frequency reference can be guided by signals from the constellation of satellites that form the global positioning system (GPS). Such frequency references are commercially available and often referred to as GPS-Disciplined oscillators (GPSDO) [22,23]. The fractional frequency uncertainty available from a GPSDO can be near or below the level of 1×10^{-11} for averaging times greater that 1 s. The uncertainty decreases approximately proportional to the averaging time on scales greater than ∼1 day, making feasible high-accuracy measurements even if they are separated by days or years.

It is important not to confuse the frequency uncertainty of the GPSDO with the linewidth it would provide for the frequency comb elements, as we might erroneously assume that an uncertainty of 1×10^{-11} provides a linewidth of a few kilohertz for the optical comb elements. In fact, the determination of the exact comb linewidth can involve many factors including the frequency noise on the free-running femtosecond laser frequency comb, the short-term (<1 s) phase-noise of the quartz oscillator in the GPSDO, the residual phase noise on a synthesizer used in converting from the quartz frequency to the repetition rate of the femtosecond laser, and the electronic servo system used in controlling the femtosecond laser comb relative to the GPSDO. The various contributions of these elements to the observed linewidth of the comb elements can be calculated, keeping in mind that the noise on the quartz crystal and microwave electronics is multiplied by the ratio of the optical and radio/microwave frequencies (e.g, something between 5×10^5 and 5×10^7). This large multiplicative factor can transform the apparently low noise of a 10 MHz oscillator (and the intermediate microwave synthesizer) into an optical linewidth that is much greater than we would naively anticipate. Nonetheless, with reasonable care and readily available components, a linewidth of the comb modes that is less than 1 MHz in the visible portion of the spectrum is readily attained. Improved radio and microwave frequency electronics could further reduce this linewidth. As noted, the linewidth scales with frequency, so a difference in linewidth by a factor of ∼2 could be expected in the two extremes of an octave-spanning spectrum. If a still narrower linewidth for the optical comb modes is required, one could employ a stabilized laser as a short time (<1 s) reference in place of the quartz oscillator. In such a case, optical linewidths from ∼100 kHz down to ∼1 Hz can be achieved [24].

6 Laser sources

Although the results we have presented were obtained with a femtosecond Ti:sapphire laser, the factors pertinent to spectrographic calibration are independent of laser type. Indeed there are several femtosecond laser combs that might be considered for use as a calibration source. The spectral range of interest (400–2000 nm) is well covered by three types of passively mode-locked lasers that employ mature technology and that have been frequency-stabilized by self-referencing. These are lasers based on Titanium-doped sapphire, Er-doped optical fiber, and Yb-doped fiber or crystal. Ti:sapphire lasers, such as the one employed here, may be carefully engineered to produce broad spectra (600–1200 nm) directly from the laser [25–27]. Still greater spectral coverage, 400–1500 nm, can be achieved by further broadening the laser in nonlinear microstructured optical fiber [28–30]. In the near infrared, femtosecond Er:fiber lasers are readily broadened in highly nonlinear fiber to provide coverage from 1000–2200 nm [31–33]. Femtosecond lasers based on Yb-doped gain media are centered at 1030 nm, spectrally almost directly between Ti:sapphire and Er lasers. The achievable pulse widths with Yb systems are comparable to Er:fiber systems (∼100 fs), and spectral broadening and frequency stabilization again can be accomplished with nonlinear fibers that cover the region of 500–1600 nm [34,35].

Despite sufficient spectral coverage by each of these lasers, the small frequency mode spacing of ∼1 GHz for Ti:sapphire and <250 MHz for Er and Yb lasers prohibits resolution of individual frequency modes, and mode filtering is necessary for use in typical astronomical spectrographs. Although this paper is aimed at mature comb technology, it should be noted that new advances on the engineering of multi-gigahertz-repetition-rate femtosecond combs may obviate the need for spectral filtering. In the quest for even greater repetition rates, lower laser intracavity peak power hinders production of broad spectral bandwidth [36]. If appropriate stabilization and laser power could be achieved, a number of ultra-high-repetition-rate frequency combs with smaller bandwidths become potential calibration sources. Finally, we note that the generation of frequency combs into the ultraviolet (200–400 nm) and mid-infrared (up to ∼4000 nm) with nonlinear optical fibers and more conventional nonlinear crystals should, in principle, allow the techniques discussed here to be extended over an even broader spectral range.

7 Conclusion

Frequency combs are a promising avenue for the calibration of astronomical spectrographs. Current comb technology requires filtering of comb modes to produce adequate mode separation that can be resolved by standard spectrographs. The parameters relevant to cavity filtering have been detailed with a demonstrated agreement between experiment and model, and a number of factors that impact COG line shifts are discussed. Beyond the compelling benefits of frequency combs as a calibration source for observational astronomy and cosmology, a laser frequency comb calibration source could positively impact several additional areas that require robust frequency sources with 10–20 GHz mode spacing. Examples include direct spectroscopy with frequency combs, remote sensing, optical and microwave waveform synthesis, high-speed coherent communications, and optical clock development. During the review process, we learned of the recent publication of an additional, closely related article [37].

The authors gratefully acknowledge Ramin Lalezeri for the data on the mirror coatings used in Figure 2; Thomas Udem, Ronald Holzwarth, Ted Hänsch, and Leo Hollberg for sharing their ideas regarding frequency combs for spectrographic calibration; and Andy Weiner for valuable discussions. Finally, we thank Nathan Newbury and Elizabeth Donley for their thoughtful comments on this manuscript. This work is a contribution of NIST, an agency of the US government, and is not subject to copyright. Partial financial support is provided by DARPA.

References

1. G.W. Marcy, R.P. Butler, Publications of the Astronomical Society of the Pacific **104**, 270 (1992)
2. C. Lovis, M. Mayor, F. Pepe, D. Queloz, S. Udry, in *Precision Spectroscopy in Astrophysics*, edited by N.C. Santos, L. Pasquini, A.C.M. Correia, M. Romaniello (2008), pp. 181–184
3. W.D. Cochran, A.P. Hatzes, M. Endl, D.B. Paulson, R.A. Wittenmyer, in *Precision Spectroscopy in Astrophysics*, edited by N.C. Santos, L. Pasquini, A.C.M. Correia, M. Romaniello (2008), pp. 175–180
4. M. Murphy et al., Mon. Not. Roy. Astr. Soc. **380**, 839 (2007)
5. P.O. Schmidt, S. Kimeswenger, H.U. Kaeufl (2007), `arXiv:0705.0763 v1`
6. J.L. Hall, Rev. Mod. Phys. **78**, 1279 (2006)
7. T.W. Hansch, Rev. Mod. Phys. **78**, 1297 (2006)
8. T. Udem, J. Reichert, R. Holzwarth, T.W. Hänsch, Opt. Lett. **24**, 881 (1999)
9. T. Sizer, IEEE J. Quant. Elect. **25**, 97 (1989)
10. T. Udem, J. Reichert, R. Holzwarth, T.W. Hänsch, Phys. Rev. Lett. **82**, 3568 (1999)
11. R.G. DeVoe, C. Fabre, K. Jungmann, J. Hoffnagle, R.G. Brewer, Phys. Rev. A **37**, 1802 (1988)
12. R.J. Jones, J.C. Diels, J. Jasapara, W. Rudolph, Opt. Commun. **175**, 409 (2000)
13. A. Schliesser, C. Gohle, T. Udem, T.W. Hänsch, Opt. Express **14**, 5975 (2006)
14. M. Born, E. Wolf, *Principles of Optics* (Cambridge University Press, 1997), Chap. 7.6
15. P.E. Ciddor, Appl. Opt. **35**, 1566 (1996)
16. K. Sarwar Abedin, N. Onodera, M. Hyodo, Appl. Phys. Lett. **73**, 1311 (1998)
17. K. Yiannopoulos, K. Vyrsokinos, D. Tsiokos, E. Kehayas, N. Pleros, G. Theophilopoulos, T. Houbavlis, G. Guekos, H. Avramopoulos, IEEE J. Quant. Elect. **40**, 157 (2004)

18. J. McFerran, E. Ivanov, A. Bartels, G. Wilpers, C. Oates, S. Diddams, L. Hollberg, Elect. Lett. **41**, 650 (2005)
19. S.A. Diddams, A.M. Weiner, V. Mbele, L. Hollberg, *LEOS Summer Topical Meetings*, Digest of the IEEE (2007), pp. 178–179
20. T.M. Fortier, A. Bartels, S.A. Diddams, Opt. Lett. **31**, 1011 (2006)
21. S. Osterman, S. Diddams, M. Beasley, C. Froning, L. Hollberg, P. MacQueen, V. Mbele, A. Weiner, *Proceedings of the SPIE 6693*, 2007, pp. 66931G
22. M. Lombardi, A. Novick, V. Zhang, *Frequency Control Symposium and Exposition, 2005. Proceedings of the IEEE International* (2005), pp. 677–684
23. J. Stone, L. Lu, P. Egan, Measure **2**, 28 (2007)
24. A. Bartels, C.W. Oates, L. Hollberg, S.A. Diddams, Opt. Lett. **29**, 1081 (2004)
25. R. Ell et al., Opt. Lett. **26**, 373 (2001)
26. A. Bartels, H. Kurz, Opt. Lett. **27**, 1839 (2002)
27. T.M. Fortier, D.J. Jones, S.T. Cundiff, Opt. Lett. **28**, 2198 (2003)
28. J.K. Ranka, R.S. Windeler, A.J. Stentz, Opt. Lett. **25**, 25 (2000)
29. V.V.R. Kanth Kumar, A.K. George, W.H. Reeves, J.C. Knight, P.S.J. Russell, F.G. Omenetto, A.J. Taylor, Opt. Express **10**, 1520 (2002)
30. J.M. Dudley, G. Genty, S. Coen, Rev. Mod. Phys. **78**, 1135 (2006)
31. J.W. Nicholson, M.F. Yan, P. Wisk, J. Fleming, F. Dimarcello, E. Monberg, A. Yablon, C. Jørgensen, T. Veng, Opt. Lett. **28**, 643 (2003)
32. F. Tauser, A. Leitenstorfer, W. Zinth, Opt. Express **11**, 594 (2003)
33. B.R. Washburn, S.A. Diddams, N.R. Newbury, J.W. Nicholson, M.F. Yan, C.G. Jørgensen, Opt. Lett. **29**, 250 (2004)
34. P. Pal, W.H. Knox, I. Hartl, M.E. Fermann, Opt. Express **15**, 12161 (2007)
35. S.A. Meyer, J.A. Squier, S.A. Diddams, Eur. Phys. J D **48**, 19 (2008)
36. *Femtosecond Optical Frequency Comb Technology*, edited by J. Ye, S.T. Cundiff (Springer, 2005)
37. C.H. Li, A.J. Benedick, P. Fendel, A.G. Glenday, F.X. Kärtner, D.F. Phillips, D. Sasselov, A. Szentgyorgyi, R.L. Walsworth, Nature **452**, 610 (2008)